Yeast genetic selections to optimize RNA decoys for transcription factor NF-κB

Laura A. Cassiday and L. James Maher III*

Department of Biochemistry and Molecular Biology, Mayo Foundation, Rochester, MN 55905

Edited by Peter B. Dervan, California Institute of Technology, Pasadena, CA, and approved February 5, 2003 (received for review October 4, 2002)

***In vitro*-selected RNA aptamers are potential inhibitors of disease-related proteins. Our laboratory previously isolated an RNA aptamer that binds with high affinity to human transcription factor NF-κB. This RNA aptamer competitively inhibits DNA binding by NF-κB *in vitro* and is recognized by its target protein *in vivo* in a yeast three-hybrid system. In the present study, yeast genetic selections were used to optimize the RNA aptamer for binding to NF-κB in the eukaryotic nucleus. Selection for improved binding to NF-κB from RNA libraries encoding (*i*) degenerate aptamer variants and (*ii*) sequences present at round 8 of 14 total rounds of *in vitro* selection yielded RNA aptamers with dramatically improved *in vivo* activity. Furthermore, we show that an *in vivo*-optimized RNA aptamer exhibits specific "decoy" activity, inhibiting transcriptional activation by its NF-κB target protein in a yeast one-hybrid assay. This decoy activity is enhanced by the expression of a bivalent aptamer. The combination of *in vitro* and *in vivo* genetic selections was crucial for obtaining RNA aptamers with *in vivo* decoy activity.**

The artificial modulation of gene expression is a major goal of modern disease therapeutics. Recently, RNA aptamers have been investigated as inhibitors of disease-related proteins (reviewed in ref. 1). *In vitro* selections using large combinatorial RNA libraries have made trivial the identification of RNA sequences that bind with high affinities to target macromolecules. However, it is not intuitive that an RNA molecule selected for binding *in vitro* likewise will bind and inhibit the target protein within the complex environment of a living eukaryotic cell. Despite this caveat, some RNA aptamers identified through *in vitro* selection have been shown to perform the desired inhibitory function when expressed in cells. For example, Famulok and colleagues (2) used *in vitro* selection to identify an RNA aptamer that inhibits the intracellular domain of the β2 integrin LFA-1. A second example of an *in vitro*-selected RNA aptamer that subsequently was shown to function *in vivo* is an inhibitory aptamer identified by Lis and colleagues (3) against the *Drosophila* B52 splicing protein.

We have been intrigued by the possibility of identifying an RNA "decoy" for a model transcription factor, human NF-κB. Such a decoy molecule might fold so as to bind at or near the DNA-binding site of the transcription factor, sequestering NF-κB and reducing its ability to activate target genes. A member of the *rel* homology protooncogene family of proteins, NF-κB exists in cells primarily as a homodimer composed of two p50 subunits [$(p50)_2$] or a heterodimer composed of one p50 and one p65 subunit (p50/p65). Both forms of NF-κB bind similar sites in duplex DNA [e.g., 5′-GGGACTTTCC (4)] but appear to activate transcription through distinct mechanisms because, unlike p65, p50 lacks a potent carboxyl-terminal transcription activation domain (5). Inhibition of NF-κB activity by the controlled expression of an RNA decoy potentially could have important therapeutic applications, because NF-κB is involved in disease processes such as inflammation, the prevention of apoptosis in tumor cells, and HIV-1 transcription (6). In fact, inhibition of NF-κB by other approaches has been shown to reduce myocardial damage after ischemia and reperfusion (7), potentiate tumor cell killing by tumor necrosis factor and radio- and chemotherapies (8), and cause spontaneous apoptosis in Epstein–Barr virus-transformed lymphoblastoid cells (9).

Our laboratory previously conducted an *in vitro* selection seeking RNA ligands for NF-κB, identifying a 31-nt RNA aptamer (α-p50) that binds with high affinity ($K_d \approx 1$ nM) to the target protein (10). Although selected for binding to the p50 homodimer form of NF-κB, the α-p50 RNA aptamer also was shown to recognize the p50/p65 heterodimer (10). In addition, α-p50 functioned as an *in vitro* decoy for NF-κB, competing with radiolabeled κB DNA for transcription factor binding (10). Furthermore, the α-p50 RNA aptamer was shown to recognize its $(p50)_2$ target within a eukaryotic nucleus (11) in a yeast three-hybrid assay (12). In this sensitive assay for detecting RNA–protein interactions, transcription of *HIS3* and *lacZ* reporter genes depends on a trimolecular interaction within the yeast nucleus (Fig. 1*A*). Fig. 1*B* shows a predicted secondary structure (13–15) of the α-p50 aptamer engrafted into the MS2 hybrid RNA required for the yeast three-hybrid system (12).

In the present study, we have further used the yeast three-hybrid system to optimize the α-p50 RNA aptamer for binding to $(p50)_2$ in the eukaryotic nucleus. Previous studies have investigated RNA aptamer modification for optimized *in vivo* expression, typically by appending rationally designed or *in vitro* selected sequences that increase aptamer expression, stability, or presentation in cells (2, 3, 16). In contrast, we now present yeast genetic selections to identify aptamer variants that show improved interaction with the target protein. This *in vivo* optimization yielded dramatic improvements in aptamer function, including subtle nucleotide changes that could not have been predicted to improve *in vivo* activity. We further show that our best optimized RNA aptamer serves as a specific RNA decoy for $(p50)_2$ in a yeast one-hybrid system. These results demonstrate that RNA decoys can be used to inhibit the function of DNA-binding proteins *in vivo* and underscore the power of combining *in vitro* and *in vivo* genetic selections in RNA engineering.

Materials and Methods

Synthesis and Cloning of Degenerate α-p50/MS2 Hybrid RNA Library. A degenerate α-p50 DNA oligonucleotide library was synthesized such that the average α-p50 variant had two to three mutations in the α-p50 DNA sequence 5′-$GATC_2TGA_3CTGT_2AT$-$A_2G_2T_2G_2C_2GATC$. The degenerate α-p50 DNA oligonucleotide library was PCR-amplified and cloned between *Xho*I and *Sph*I sites of pJ714, a version of pIIIA/MS2–2 (12) encoding MS2 hybrid RNAs with a GC "clamp" flanking the inserted sequence.

Cloning of Early-Round *in Vitro* Selection RNA Library. Sixty-nucleotide RNA sequences present at round 8 of the prior 14-round *in vitro* selection for $(p50)_2$ RNA ligands (10) were reverse-transcribed, PCR-amplified, and cloned between *Xho*I and *Sph*I sites of pJ713, a version of pIIIA/MS2–2 (12) without a GC clamp flanking the inserted sequence.

This paper was submitted directly (Track II) to the PNAS office.

Abbreviations: GAL4AD, yeast GAL4 transcriptional activation domain; 3-AT, 3-amino-1,2,4-triazole; snRNA, small nuclear RNA.

*To whom correspondence should be addressed at: Department of Biochemistry and Molecular Biology, Guggenheim 16, Mayo Foundation, 200 First Street SW, Rochester, MN 55905. E-mail: maher@mayo.edu.

 www.pnas.org/cgi/doi/10.1073/pnas.0736013100

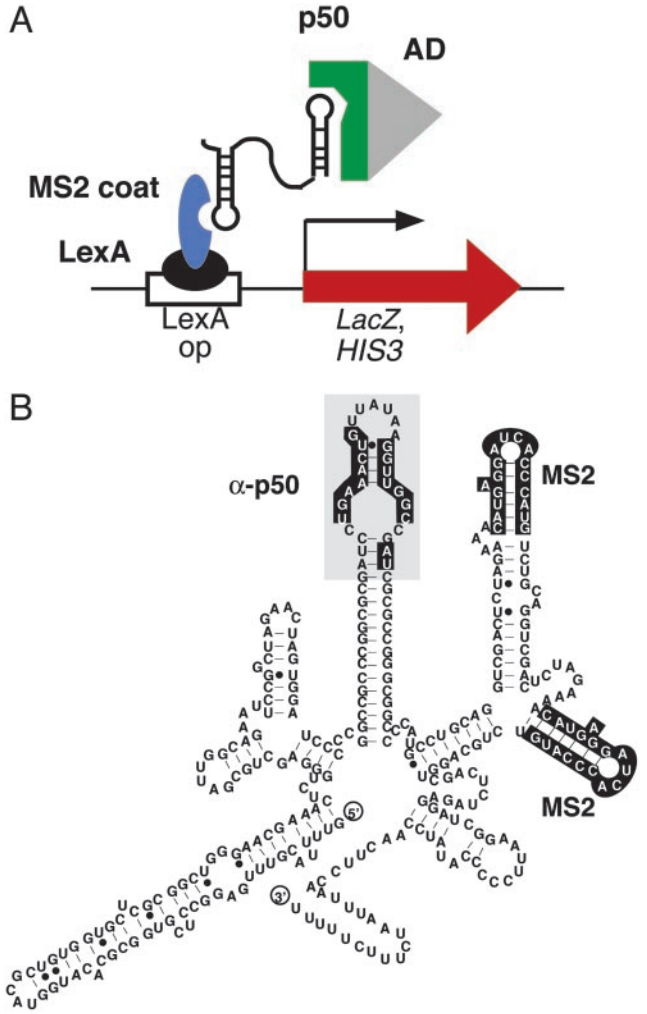

Fig. 1. (*A*) The yeast three-hybrid system. Transcription of *lacZ* and *HIS3* reporter genes (red) depends on a trimolecular interaction between hybrid protein 1 (LexA/MS2 coat protein fusion, black/blue), a hybrid RNA composed of the MS2 recognition sequence and the α-p50 aptamer sequence, and hybrid protein 2 (GAL4AD/p50, gray/green). (*B*) Predicted secondary structure of the initial α-p50/MS2 hybrid RNA. The *in vitro*-selected α-p50 RNA aptamer domain is shaded, with highlighting of nucleotides previously shown to be important for $(p50)_2$ binding (10). MS2 coat protein recognition sequences are also highlighted.

Hybrid Protein Constructs. The yeast GAL4 transcriptional activation domain (GAL4AD)/p50 hybrid protein yeast expression plasmid used in yeast three-hybrid screens encodes human p50 amino acid residues 18–502 downstream of the yeast GAL4AD in the yeast shuttle vector pGAD424 (CLONTECH). For decoy assays, the alcohol dehydrogenase-1 promoter–GAL4AD-p50 cassette from the GAL4AD/p50 construct in pGAD424 was PCR-amplified, appending 5′ *Apa*I and 3′ *Aat*II restriction sites for cloning into the ARS4/Cen6 vector pEXP-AD502 (CLONTECH). The GAL4AD/Sp1 hybrid protein yeast expression plasmid was generated in a similar fashion, by cloning an alcohol dehydrogenase-1-GAL4AD-Sp1 cassette from pGAD424 (CLONTECH) into pEXP-AD502 (CLONTECH). The resulting plasmid encodes the 167 carboxyl-terminal residues of human Sp1 downstream of the yeast GAL4AD.

Yeast Three-Hybrid Screens for Optimized α-p50 RNAs. The host yeast strain L40-coat (12) expressing the GAL4AD/p50 hybrid protein was transformed with three-hybrid RNA plasmid libraries encoding (*i*) a degenerate α-p50 RNA library or (*ii*) an early-round *in vitro* selection RNA library. The transformation mixtures were plated on selective medium containing 3 mM 3-amino-1,2,4-triazole (3-AT). An estimated 3×10^5 plasmid sequences were screened in each case. Aptamer-encoding plasmids were isolated from *HIS3*- and *lacZ*-positive transformants as described (17) and retransformed into fresh L40-coat expressing GAL4AD/p50 to confirm phenotypes. True positive clones then were sequenced to analyze selected hybrid RNAs.

Reporter Gene Assays. For the *HIS3* reporter gene assay, yeast strains were grown to an optical density at 600 nm of ≈1.0 and diluted for plating of 1,000-cell spots on selective medium containing a 3-AT gradient over the concentration range specified in the figure legends. The *lacZ* reporter gene assay was conducted by using the substrate *o*-nitrophenyl β-D-galactopyranoside as described (18). Three to six independent transformants were assayed for each yeast strain.

Determination of *in Vitro* RNA Affinity and *in Vivo* RNA Accumulation. RNA affinities for $(p50)_2$ were determined by using a nitrocellulose filter-binding assay. RNA aptamers 1 (5′-$GAUC_2UGA_3CUGU_4A_2G_2U_2G_2C_2GAUC$) and 6 (5′-$CAUAC\text{-}U_2GA_3CUGUA_2G_2U_2G_2CGUAUG$) were purchased from Dharmacon Research (Lafayette, CO), deprotected according to the protocol suggested by the supplier, and purified by denaturing PAGE and elution. Purified RNAs were radiolabeled with [γ-^{32}P]ATP by using T4 polynucleotide kinase (New England Biolabs). $(p50)_2$ protein (amino acid residues 39–363) was expressed in *Escherichia coli* and purified as described (19).

Binding reactions consisted of a known concentration (0.85 nM) of the indicated radiolabeled RNA aptamer and increasing concentrations (50 pM to 5 μM) of recombinant, purified $(p50)_2$. $(p50)_2$ and labeled RNA 1 or 6 were incubated in binding buffer (10 mM Hepes, pH 7.5/100 mM NaCl/1 mM DTT) for 30 min at 25°C, filtered over nitrocellulose membranes, and quantitated by scintillation counting. Estimates of K_d were obtained by least-squares curve-fitting of binding isotherms (10).

To compare the accumulation in yeast of hybrid RNAs 1, 4, and 6, total RNA was extracted from yeast three-hybrid strains as described (20). Northern blot analysis was conducted as described (11), simultaneously hybridizing with radiolabeled oligonucleotide probes complementary to the RNase P RPR1 leader (5′-$AGCAC_2ACAGCGTAC_2ATGT$) and to the U6 small nuclear RNA (snRNA) (5′-$TC_2T_2ATGCAG_4A_2CTGC$). Radioactivity was detected and analyzed by storage phosphor technology.

RNA Decoy Assays. For decoy assays, hybrid proteins were expressed from the ARS4/Cen6 vector pEXP-AD502 (CLONTECH) in a κB yeast one-hybrid dual reporter strain (11). RNA sequences were cloned between the *Xho*I and *Sph*I restriction sites of pJ903, a version of pIIIA/MS2–2 (12) that carries a *leu2-d* marker in place of the *URA3* marker, to express ≈300-nt hybrid RNA 6, identical to RNA 6 expressed in the three-hybrid system. Briefly, pJ903 was constructed by homologous *in vivo* recombination between pJ713 and a PCR product encoding the *leu2-d* sequence from pBS24-ΔAB6 (kindly provided by David Brow, University of Wisconsin, Madison) flanked on both sides by 40-nt regions of homology to 5′ and 3′ *URA3* sequences.

Results

Degenerate α-p50/MS2 Hybrid RNA Library Screen. Previously, we tested our *in vitro* selected α-p50 RNA aptamer in the yeast three-hybrid system and showed that the aptamer was recognized by its target protein, NF-κB [$(p50)_2$], in a eukaryotic nucleus (11). We wanted to use yeast genetic selections to optimize the α-p50 RNA aptamer for $(p50)_2$ recognition in yeast, with the ultimate goal of identifying an RNA decoy for $(p50)_2$ that functions *in vivo*. As a starting point, we reasoned that by

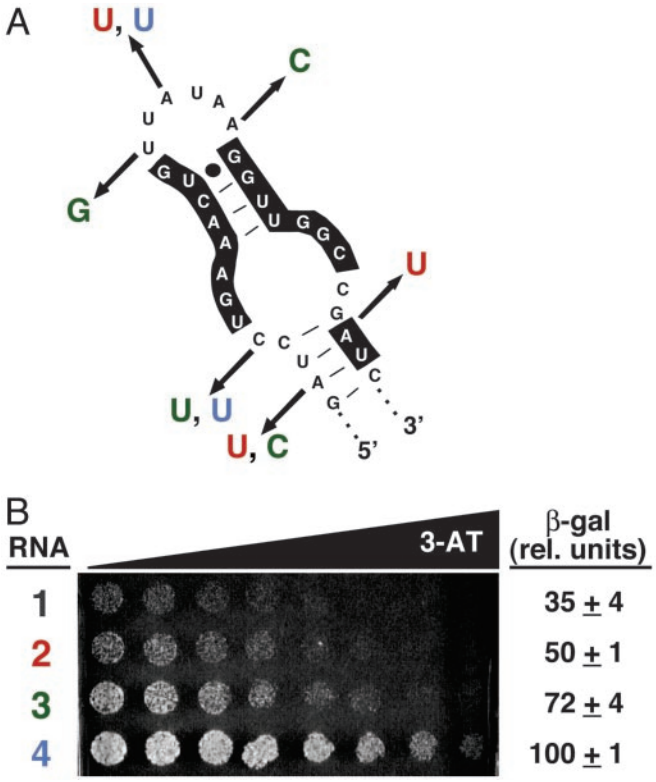

Fig. 2. *In vivo* optimization of degenerate α-p50 aptamers. (*A*) Nucleotide changes selected for improved $(p50)_2$ binding in yeast. Shown is the *in vitro*-selected α-p50 aptamer (1). Colored nucleotides indicate the combinations of mutations found to improve aptamer–$(p50)_2$ interaction in yeast, yielding RNAs 2 (red), 3 (green), and 4 (blue). Nucleotides previously shown to be important for $(p50)_2$ binding (10) are highlighted. (*B*) Yeast three-hybrid system *HIS3* and *lacZ* reporter gene assays. Growth assay for *HIS3* expression is on selective medium containing a gradient of up to 4 mM 3-AT. β-Galactosidase data reflect three independent transformants for each yeast strain.

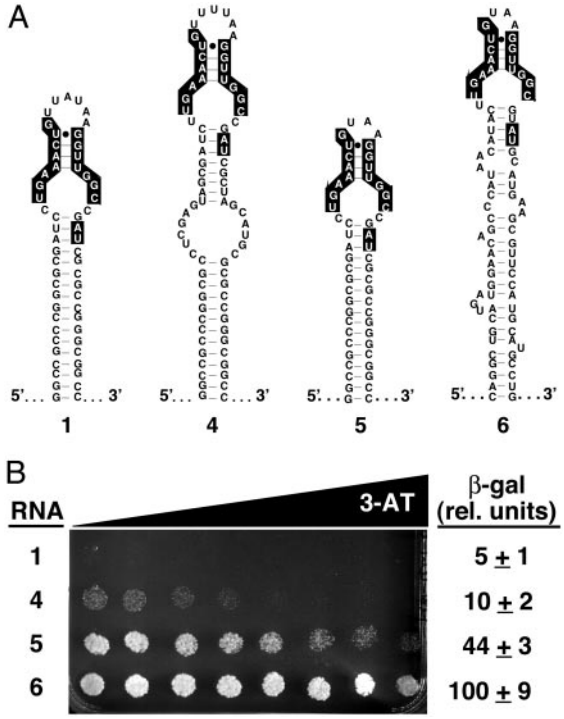

Fig. 3. A yeast-optimized RNA aptamer selected from an early-round *in vitro* selection library exhibits drastically improved binding to NF-κB. (*A*) Predicted secondary structures of α-p50 RNA aptamer domains selected *in vitro* and in yeast: 1, *in vitro*-selected (α-p50 + GC clamp); 4, (α-p50 + GC clamp) variant 4 selected in yeast from degenerate library (Fig. 2); 5, (α-p50 + GC clamp + tetraloop); 6, α-p50 aptamer selected in yeast from a library encoding sequences present at round 8 of the 14-round *in vitro* selection. Nucleotides previously shown to be important for $(p50)_2$ binding (10) are highlighted. (*B*) Yeast three-hybrid system *HIS3* and *lacZ* reporter gene assays. Growth assay for *HIS3* expression is on selective medium containing a gradient of up to 5 mM 3-AT. β-Galactosidase data reflect three independent transformants for each yeast strain.

changing only one or a few nucleotides within the α-p50 RNA aptamer framework, we might achieve improved *in vivo* activity. To this end, a degenerate α-p50 DNA library was synthesized such that the average α-p50 variant carried two to three mutations. The resulting 31-bp, double-stranded, degenerate α-p50 DNA library was cloned into the three-hybrid system RNA expression vector and transformed into the yeast three-hybrid host strain L40-coat (12) expressing GAL4AD/p50. Degenerate α-p50 hybrid RNA sequences were screened for improved *in vivo* binding to $(p50)_2$ by plating the transformation mixture on selective medium containing a higher 3-AT concentration than that tolerated by the yeast strain coexpressing GAL4AD/p50 with the original, *in vitro*-selected α-p50 RNA aptamer. This procedure seeks hybrid RNAs that induce higher levels of *HIS3* reporter gene expression than previously achieved.

Reselection yielded improved aptamers. After confirming and sequencing, three α-p50 variants were identified that show improved $(p50)_2$ binding in the yeast three-hybrid system (Fig. 2). Combinations of mutations found to improve the aptamer–$(p50)_2$ interaction in yeast are indicated in Fig. 2*A*. With the exception of one A-to-U mutation in RNA 2 (Fig. 2, red), all mutations occurred outside of the region previously shown to be important for $(p50)_2$ binding to the original *in vitro*-selected α-p50 aptamer (10). Interestingly, at three nucleotide positions, mutations occurred in two of the three selected sequences (Fig. 2*A*), suggesting that these might be important nucleotide changes for improving the aptamer–$(p50)_2$ interaction *in vivo*. As shown in Fig. 2*B*, yeast three-hybrid strains expressing RNAs 2, 3, and 4 exhibited enhanced *HIS3* and *lacZ* reporter gene expression, as compared with the original *in vitro*-selected α-p50 aptamer (RNA 1). In particular, mutating only two nucleotide positions within the α-p50 sequence (RNA 4, blue) resulted in significantly increased growth on a 3-AT gradient plate and ≈3-fold increased β-galactosidase levels, supporting the idea that subtle changes in α-p50 aptamer sequence can greatly improve *in vivo* binding activity.

Early-Round *in Vitro* Selection RNA Library Screen. We further reasoned that sequences present midway through the *in vitro* selection for $(p50)_2$ RNA aptamers (10) might actually show improved *in vivo* activity compared with the α-p50 aptamer that ultimately prevailed after 14 rounds of *in vitro* selection. Therefore, 60-nt RNA sequences present at round 8 of the 14-round *in vitro* selection for $(p50)_2$ RNA ligands (10) were reverse-transcribed, PCR-amplified, and cloned into the yeast three-hybrid system RNA vector. This early-round *in vitro* selection library then was transformed into the yeast three-hybrid host strain L40-coat (12) expressing GAL4AD/p50. As before, to select for α-p50 hybrid RNA sequences with improved *in vivo* binding to $(p50)_2$, the transformation mixture was plated on selective medium containing a higher 3-AT concentration than that tolerated by the yeast strain coexpressing GAL4AD/p50 with the original, *in vitro* selected α-p50 RNA aptamer.

Analysis of selected transformants revealed a single RNA sequence (Fig. 3*A*, RNA 6). Interestingly, the sequence included the nucleotides previously shown to be important for $(p50)_2$ binding to the original *in vitro*-selected α-p50 aptamer (10).

However, the remainder of the sequence appears to have evolved independently from the α-p50 RNA aptamer that had prevailed originally *in vitro*. The most striking change is the presence of a 5′-GUAA tetraloop in place of the 7-nt terminal loop of α-p50 (Fig. 3*A*, compare RNAs 1 and 6). This tetraloop modification may enhance the proper *in vivo* folding of RNA 6. Other more subtle changes from the *in vitro*-selected α-p50 sequence are also evident, including a C-to-U change in the left side of the internal unpaired region of α-p50 that also was selected in the degenerate RNA library screen (Figs. 2*A* and 3*A*, RNA 4) and the deletion of a C residue from the right side of the internal unpaired region of α-p50. In addition, the RNA 6 sequence provided its own selected "clamp" in place of the engineered GC clamp found to aid the proper folding/presentation of RNA 1 (11).

As shown in Fig. 3*B*, the yeast three-hybrid strain expressing RNA 6 showed dramatically enhanced *HIS3* and *lacZ* reporter gene expression, as evidenced by increased growth on a 3-AT gradient plate and β-galactosidase levels that were ≈20- and ≈10-fold higher, respectively, than for RNA 1 or degenerate RNA 4. We wondered whether the increased $(p50)_2$-binding activity of RNA 6 was due solely to the presence of the GUAA tetraloop. To answer this question, a sequence was cloned into the hybrid RNA vector to express a version of RNA 1 with a tetraloop substituted in place of the terminal loop of α-p50 (Fig. 3*A*, RNA 5). When transformed into the yeast three-hybrid strain expressing GAL4AD/p50, hybrid RNA 5 shows increased $(p50)_2$ binding in *HIS3* and *lacZ* reporter assays compared with RNAs 1 and 4 (Fig. 3*B*), indicating that the tetraloop makes an important contribution to the improved *in vivo* binding of RNA 6 to $(p50)_2$. However, the yeast three-hybrid strain expressing RNA 6 shows increased growth on a 3-AT gradient plate and ≈2-fold-higher β-galactosidase levels than the strain expressing RNA 5, suggesting that additional sequence features present in RNA 6 significantly enhance its *in vivo* activity.

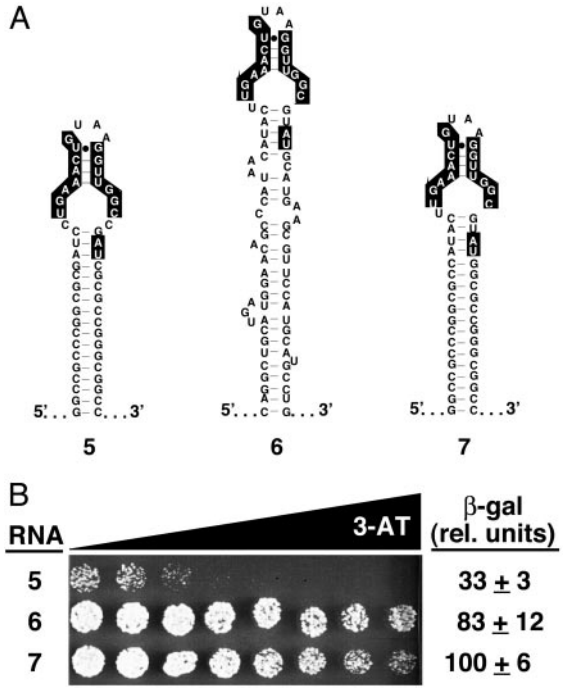

Fig. 4. Yeast-selected RNA clamp is not essential. (*A*) Predicted secondary structures of α-p50 RNA aptamers 5, 6, and 7 (RNA 6 with GC clamp substituted for yeast three-hybrid-selected clamp). Nucleotides previously shown to be important for $(p50)_2$ binding (10) are highlighted. (*B*) Yeast three-hybrid system *HIS3* and *lacZ* reporter gene assays. Growth assay for *HIS3* expression is on selective medium containing a gradient of up to 8 mM 3-AT. β-Galactosidase data reflect three independent transformants for each yeast strain.

Contribution of *in Vivo*-Selected RNA Clamp. The predicted secondary structure of RNA 6, selected from an early-round *in vitro* selection RNA library, suggests the presence of a double-stranded clamp structure different from the GC clamp engineered into RNAs 1–5 (see Fig. 3*A*). Thus, we wondered whether this potential clamp contributed to the improved activity of RNA 6 in the yeast three-hybrid system. To answer this question, the selected clamp of RNA 6 was replaced with the GC clamp sequence of RNA 5, resulting in RNA 7 (Fig. 4*A*). This RNA then was compared with RNAs 5 and 6 for binding to $(p50)_2$ in the yeast three-hybrid system. 3-AT gradient plate and β-galactosidase assays revealed that, within error, RNA 7 binds $(p50)_2$ comparably to RNA 6 (Fig. 4*B*), suggesting the selected clamp of RNA 6 does not contribute to its improved $(p50)_2$ binding. Intriguingly, although RNAs 5 and 7 differ at only four nucleotide positions, none of which are predicted to affect RNA folding, yeast three-hybrid strains expressing RNA 7 yield ≈3-fold-higher β-galactosidase reporter gene activity than strains expressing RNA 5 (Fig. 4*B*). These subtle changes could not have been rationally designed or predicted, highlighting the power of yeast genetic selections for RNA aptamer optimization.

***In Vitro* RNA Affinity and *in Vivo* RNA Accumulation.** In an attempt to discover the basis for improved $(p50)_2$ binding by RNA 6 in yeast three-hybrid assays, the affinities of RNAs 1 and 6 for $(p50)_2$ were compared *in vitro* (Fig. 5*A*). Nitrocellulose filter experiments measuring the binding of radiolabeled RNA competitors 1 or 6 to increasing concentrations of recombinant, purified $(p50)_2$ resulted in the binding curves shown in Fig. 5*A*. Curve-fitting of binding isotherms (10) yielded equilibrium dissociation constant (K_d) estimates for RNAs 1 and 6 binding to $(p50)_2$ of 6.8 ± 4 nM and 5.4 ± 2 nM, respectively. Likewise, RNAs 1 and 6 were found to bind comparably to the p50/p65 form of NF-κB, with K_d values of 17.4 ± 6 nM and 22.1 ± 7 nM, respectively (data not shown). Within error, the *in vitro* affinities of RNAs 1 and 6 for $(p50)_2$ were indistinguishable, suggesting that RNA 6 was not selected from the yeast three-hybrid screen on the basis of improved affinity for the $(p50)_2$ target protein.

To examine the accumulation of RNAs 1, 4, and 6 in yeast, a Northern blot analysis of total yeast RNA was conducted, probing simultaneously with radiolabeled oligonucleotides complementary to the RNase P RPR1 leader (present in all of the hybrid RNAs) and to the U6 snRNA as an internal control. As shown in Fig. 5*B*, although there is a slight increase in RNA levels

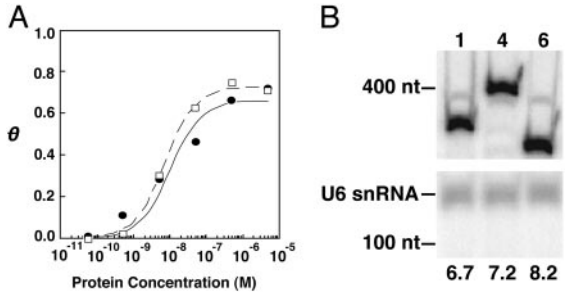

Fig. 5. Yeast-optimized α-p50 RNA aptamers do not exhibit increased $(p50)_2$ affinity *in vitro* or improved accumulation in yeast. (*A*) Plot of θ [the fractional saturation of radiolabeled RNA 1 (●) or 6 (□)] vs. $(p50)_2$ concentration (M) for increasing concentrations of $(p50)_2$ protein, as determined by nitrocellulose filter-binding assays. Curve fit is to equation 1 in ref. 10. (*B*) Northern blot comparing accumulation of RNAs 1, 4, and 6 in yeast. Yeast total RNA was extracted and assayed by Northern blotting, probing with radiolabeled oligonucleotides complementary to the RNase P RPR1 leader and to the U6 snRNA. Mobilities of DNA size markers are indicated. At the bottom of each lane is shown the signal intensity of RNA 1, 4, or 6 relative to the U6 snRNA internal control.

BIOCHEMISTRY

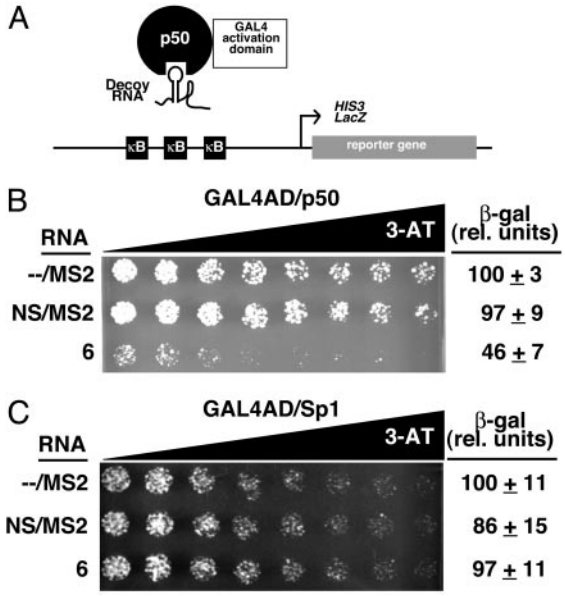

Fig. 6. Yeast-optimized RNA 6 functions as a specific $(p50)_2$ decoy in yeast. (*A*) Yeast one-hybrid decoy assay system. Binding of an RNA decoy to GAL4AD/p50 blocks binding of the fusion protein to κB sites on DNA, thus reducing transcription of *HIS3* and *lacZ* reporter genes. (*B*) $(p50)_2$ one-hybrid decoy system *HIS3* and *lacZ* reporter gene assays. Growth assay for *HIS3* expression is on selective medium containing a gradient of up to 0.5 mM 3-AT. β-Galactosidase data reflect six independent transformants for each yeast strain. (*C*) Negative control Sp1 one-hybrid decoy system *HIS3* and *lacZ* reporter gene assays.

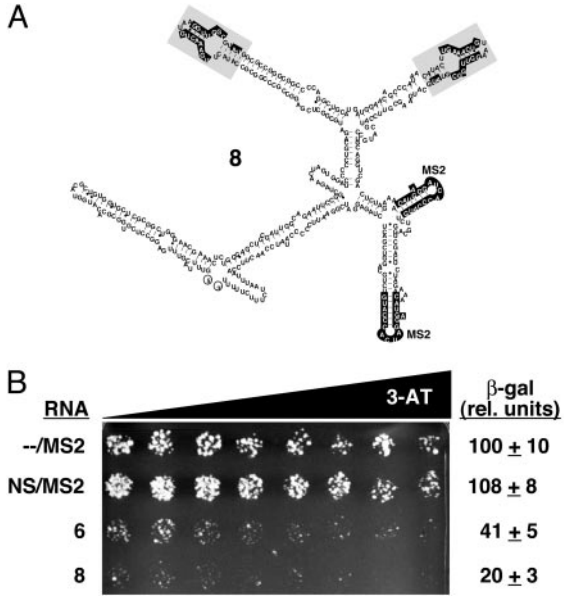

Fig. 7. Effect of increasing intracellular concentration of RNA 6. (*A*) Predicted secondary structure of bivalent RNA 8. The *in vitro*-selected α-p50 RNA aptamer domain is shaded, with highlighting of nucleotides previously shown to be important for $(p50)_2$ binding (10). MS2 coat protein-recognition sequences also are highlighted. (*B*) *HIS3* and *lacZ* reporter assays showing that RNA 8 exhibits an ≈2-fold-enhanced decoy effect compared with RNA 6. Growth assay for *HIS3* expression is on selective medium containing a gradient of up to 0.5 mM 3-AT. β-Galactosidase data reflect six independent transformants for each yeast strain.

with increasing yeast three-hybrid activity ([RNA] $1 < 4 < 6$), the difference in RNA accumulation does not appear to be sufficient to explain the ≈20-fold increased activity of RNA 6 compared with RNA 1 (Fig. 3*B*). Thus, variable(s) other than increased $(p50)_2$ affinity or RNA accumulation are implicated in the selection of RNA 6 from the early-round *in vitro* selection library. Other possible factors that may explain the improved *in vivo* $(p50)_2$ binding by RNA 6 include improved folding, enhanced nuclear localization, or increased specificity for the target protein vs. nonspecific partners within the yeast cell.

RNA Decoy Assays. We wanted to determine whether optimized RNA 6 could function as a competitive RNA decoy for its transcription factor target in yeast. To this end, we generated a yeast one-hybrid decoy assay system (Fig. 6*A*). Binding of an RNA decoy to the DNA-binding site of $(p50)_2$ should block access of the transcription factor to DNA, thereby reducing expression of *HIS3* and *lacZ* reporter genes. When constructs encoding (*i*) only MS2-coat protein recognition sites (−/MS2), (*ii*) a nonspecific aptamer/MS2 hybrid RNA (NS/MS2), or (*iii*) RNA 6 were transformed into the yeast one-hybrid strain and assayed, only RNA 6 showed a decoy effect, as evidenced by decreased survival on 3-AT gradient plates and by ≈55% reduced β-galactosidase levels (Fig. 6*B*). To ensure that the decoy effect caused by RNA 6 was specific for $(p50)_2$, a second yeast one-hybrid decoy strain was constructed with three copies of the Sp1-binding site upstream of *HIS3* and *lacZ* reporter genes and expressing GAL4AD/Sp1. When this yeast one-hybrid strain was transformed with the same three-hybrid RNA constructs and assayed for *HIS3* and *lacZ* reporter gene expression, none of these RNAs exhibited a decoy effect (Fig. 6*C*). This result is consistent with the notion that RNA 6 is a specific decoy for $(p50)_2$.

Effect of Increasing Intracellular Concentration of RNA 6. To investigate the effect of increasing aptamer concentration upon RNA decoy activity, a "bivalent" aptamer (RNA 8; Fig. 7*A*) containing two copies of the optimized α-p50 domain was cloned. A GC clamp and the yeast three-hybrid-selected clamp of RNA 6 were used to aid in the folding and/or presentation of the aptamer domains within hybrid RNA 8. When RNA 8 was expressed in the yeast one-hybrid decoy assay system shown in Fig. 6*A*, this strain showed decreased survival on a 3-AT gradient plate and ≈2-fold-decreased β-galactosidase activity compared with RNA 6 (Fig. 7*C*). This result shows that the optimized α-p50 RNA aptamer exhibits a dose-dependent effect upon $(p50)_2$ DNA binding and implies that by increasing the concentration of the optimized α-p50 aptamer, a greater decoy effect may be achieved.

Discussion

***In Vivo* RNA Aptamer Optimization.** After showing that an *in vitro*-selected RNA aptamer to human transcription factor NF-κB is recognized in the yeast nucleus by its target protein (11), we now have used yeast genetic selections to optimize this RNA–protein interaction *in vivo*. Screening a library of degenerate α-p50 hybrid RNAs for improved binding to $(p50)_2$ in a yeast three-hybrid system resulted in the selection of three α-p50 variants with markedly improved *in vivo* activity (Fig. 2). This result demonstrated that even modest changes in nucleotide sequence [e.g., two nucleotide "mutations" in RNA 4 (Fig. 2)] can have a significant impact on *in vivo* binding of an RNA aptamer to its protein target.

In addition, we screened RNA sequences present at round 8 of the original 14-round *in vitro* selection for RNA ligands for $(p50)_2$ (10), again seeking improved binding to the target protein in the yeast three-hybrid system. A selected sequence (RNA 6) retains a conserved region of the α-p50 aptamer but appears to have evolved independently from the α-p50 RNA aptamer that ultimately prevailed after 14 rounds of *in vitro* selection (Fig. 3). RNA 6 shows dramatically improved *in vivo* activity relative to both the original *in vitro*-selected α-p50 aptamer (RNA 1) and

RNA 4 selected from the degenerate α-p50 hybrid RNA library (Fig. 3). Our results show that during the course of *in vitro* selection, sequences may become extinct that actually would function better within the much more complex environment of the eukaryotic cell. Thus, by complementing the massive screening capability of a first stage of *in vitro* selections with a second stage of yeast genetic selections, optimized RNA aptamers with improved *in vivo* activity may be identified.

Factors Driving Improved *in Vivo* RNA Aptamer Activity. Factors that may influence the activity of RNA aptamers *in vivo* include proper RNA folding, intracellular accumulation, subcellular localization, and specificity for the target protein in the face of immense competition from other cellular factors. In our system, the single most important aptamer modification for improved $(p50)_2$ binding was the substitution of a tetraloop in place of the 7-nt terminal loop of RNA 1 (Fig. 3). This modification resulted in >8-fold-increased β-galactosidase levels in a yeast three-hybrid system *lacZ* reporter gene assay (Fig. 3*B*). The tetraloop sequence, which is known to preferentially form U turns, may aid in the proper folding of the α-p50 aptamer sequence within the much larger (≈300-nt) hybrid RNA required for the yeast three-hybrid system. Interestingly, initial *in vitro* experiments assessing α-p50/MS2 hybrid RNA binding to $(p50)_2$ suggested that the substitution of a tetraloop for the *in vitro*-selected α-p50 7-nt terminal loop adversely affected binding of the RNA aptamer to $(p50)_2$ (11). Furthermore, when RNAs 1, 4, and 6 were transcribed *in vitro*, folded, radiolabeled, and electrophoresed under native conditions, each of the RNAs migrated as a single major species (data not shown), suggesting that these ≈300-nt hybrid RNAs are each similarly capable of adopting a single, preferred structure *in vitro*. These observations suggest that the tetraloop sequence may be particularly important for proper hybrid RNA folding in the context of the cell, again highlighting the differences in selective pressures encountered *in vivo* vs. *in vitro*.

Increased affinity for the $(p50)_2$ target protein does not appear to have contributed significantly to enhanced aptamer activity, because the *in vitro* affinities of RNAs 1 and 6 for $(p50)_2$ are indistinguishable (Fig. 5*A*). Increased intracellular RNA stability and/or accumulation also do not appear to be significant contributing factors, because the levels of RNAs 1, 4, and 6 within the yeast cell are comparable (Fig. 5*B*). Particularly enigmatic is the ≈3-fold-increased β-galactosidase levels in a yeast three-hybrid strain expressing RNA 7 vs. RNA 5, because both hybrid RNAs contain tetraloop and GC clamp sequences and differ only at four nucleotide positions. Perhaps these subtle nucleotide changes, one of which also was selected in the degenerate α-p50 library screen (Fig. 2*A*), are sufficient to allow discrimination against illegitimate protein partners that compete with the intended $(p50)_2$ target.

Transcription Factor Decoy Activity of RNA 6. The *in vivo* RNA optimizations described above were undertaken in an attempt to identify an RNA ligand that binds $(p50)_2$ with sufficient *in vivo* affinity and specificity to function as a transcription factor decoy. In a yeast one-hybrid system, optimized RNA 6 was shown to exhibit decoy activity for the p50 homodimer form of NF-κB but not for a nonspecific transcription factor, Sp1 (Fig. 6). This decoy activity resulted in decreased expression of *HIS3* and *lacZ* reporter genes (Fig. 6*B*). The α-p50 RNA aptamer apparently binds to $(p50)_2$ with a 1:1 stoichiometry in solution (21), suggesting the aptamer targets the DNA-binding groove of the transcription factor. Binding of κB DNA and α-p50 RNA to overlapping sites would explain the observed *in vitro* (10, 11) and *in vivo* (Fig. 6*B*) competition of the RNA aptamer with κB DNA for $(p50)_2$ binding. The decoy activities of RNAs 1, 4, and 6 in the yeast one-hybrid system correlated with the strengths of interaction with $(p50)_2$ in the three-hybrid system (data not shown), indicating that yeast three-hybrid system aptamer optimization was key to achieving a strong RNA decoy effect.

Unlike the sensitive yeast three-hybrid system, the activity of α-p50 RNA aptamers in the yeast one-hybrid system appears to highly depend on RNA concentration. Initial decoy assays expressing hybrid RNA 6 from the 2-μm vector used in yeast three-hybrid selections [a version of pIIIA/MS2–2 (12)] resulted in sporadic decoy activity that depended on slight differences in RNA accumulation among individual yeast transformants (unpublished observations). By increasing the level of RNA expression ≈2-fold (unpublished observations) through the use of an RNA expression vector bearing a *leu2-d* marker (22), a reproducible decoy affect was achieved (Fig. 6*B*). By further increasing the concentration of RNA 6 through the expression of a bivalent aptamer (RNA 8; Fig. 7*A*), the $(p50)_2$ decoy effect was enhanced ≈2-fold compared with the analogous "monovalent" aptamer, RNA 6 (Fig. 7*B*). This result highlights the potential to completely saturate the DNA-binding site of $(p50)_2$ by further increasing the intracellular concentration of α-p50 RNA aptamers.

Implications. The occurrence of apparent natural RNA decoys (23) suggests the possibility of expressing therapeutic decoy RNAs in cells to modulate gene expression (24). Such RNA decoys might offer certain advantages over RNA-based knockdown strategies that require many cellular components for RNA processing and activity [i.e., RNA interference technologies (25)]. In the case of RNA interference for cancer, tumor cell variants likely will overcome such therapies by mutation of any of a number of components in the nonessential RNA interference-processing pathway. Similarly, antiviral RNA interference therapies will be sensitive to point mutations in the target RNA sequence. It may be more difficult for diseased cells to evolve resistance to RNA decoy therapies. We have shown that genetic selections in yeast can dramatically improve *in vivo* RNA aptamer function relative to what was achieved after *in vitro* selection alone. It will be fascinating to determine whether optimization in one eukaryotic system will lead to improved aptamer performance in other eukaryotic cells.

This work is respectfully dedicated to the memory of Frank M. Rusnak. We thank Marvin Wickens, Stanley Fields, David Brow, Gourisanker Ghosh, and Claus Scheidereit for materials and advice and W. Scott Moye-Rowley, Joseph Gera, Wendy Olivas, Roy Parker, and Grazia Isaya for technical suggestions. We acknowledge the excellent technical assistance of Jeff Zimmerman. This work was supported by the Mayo Foundation and American Cancer Society Grant GMC-98585. L.A.C. is a Howard Hughes Medical Institute Predoctoral Fellow.

1. Sullenger, B. A. & Gilboa, E. (2002) *Nature* **418,** 252–258.
2. Blind, M., Kolanus, W. & Famulok, M. (1999) *Proc. Natl. Acad. Sci. USA* **96,** 3606–3610.
3. Shi, H., Hoffman, B. E. & Lis, J. T. (1999) *Proc. Natl. Acad. Sci. USA* **96,** 10033–10038.
4. Kunsch, C., Ruben, S. M. & Rosen, C. A. (1992) *Mol. Cell. Biol.* **12,** 4412–4421.
5. Fujita, T., Nolan, G. P., Ghosh, S. & Baltimore, D. (1992) *Genes Dev.* **6,** 775–787.
6. Baeuerle, P. A. & Baltimore, D. (1996) *Cell* **87,** 13–20.
7. Morishita, R., Sugimoto, T., Aoki, M., Kida, I., Tomita, N., Moriguchi, A., Maeda, K., Sawa, Y., Kaneda, Y., Higaki, J., *et al.* (1997) *Nat. Med.* **3,** 894–899.
8. Beg, A. A. & Baltimore, D. (1996) *Science* **274,** 782–784.
9. Cahir-McFarland, E. D., Davidson, D. M., Schauer, S. L., Duong, J. & Kieff, E. (2000) *Proc. Natl. Acad. Sci. USA* **97,** 6055–6060.
10. Lebruska, L. L. & Maher, L. J., III (1999) *Biochemistry* **38,** 3168–3174.
11. Cassiday, L. A. & Maher, L. J., III (2001) *Biochemistry* **40,** 2433–2438.
12. SenGupta, D. J., Zhang, B., Kraemer, B., Pochart, P., Fields, S. & Wickens, M. (1996) *Proc. Natl. Acad. Sci. USA* **93,** 8496–8501.
13. Jaeger, J. A., Turner, D. H. & Zuker, M. (1989) *Proc. Natl. Acad. Sci. USA* **86,** 7706–7710.
14. Jaeger, J. A., Turner, D. H. & Zuker, M. (1989) *Methods Enzymol.* **183,** 281–306.
15. Zuker, M. (1989) *Science* **244,** 48–52.
16. Martell, R. E., Nevins, J. R. & Sullenger, B. A. (2002) *Mol. Ther.* **6,** 30–34.
17. CLONTECH (1999) *Yeast Protocols Handbook PT3024–1* (CLONTECH, Palo Alto, CA), pp. 34–36.
18. Zhang, X. & Moye-Rowley, W. S. (2001) *J. Biol. Chem.* **276,** 47844–47852.
19. Ghosh, G., Duyne, G. V., Ghosh, S. & Sigler, P. (1995) *Nature* **373,** 303–310.
20. Caponigro, G., Muhlrad, D. & Parker, R. (1993) *Mol. Cell. Biol.* **13,** 5141–5148.
21. Cassiday, L. A., Lebruska, L. L., Benson, L. M., Naylor, S., Owen, W. G. & Maher, L. J. (2002) *Anal. Biochem.* **306,** 290–297.
22. Erhart, E. & Hollenberg, C. P. (1983) *J. Bacteriol.* **156,** 625–635.
23. Cassiday, L. A. & Maher, L. J., III (2002) *Nucleic Acids Res.* **30,** 4118–4126.
24. Ishizaki, J., Nevins, J. R. & Sullenger, B. A. (1996) *Nat. Med.* **2,** 1386–1389.
25. Hannon, G. J. (2002) *Nature* **418,** 244–251.